Title	Influence of disturbances and environmental changes on albedo in tropical peat ecosystems
Author(s)	Ohkubo, Shinjiro; Hirano, Takashi; Kusin, Kitso
Citation	Agricultural and forest meteorology, 301, 108348 https://doi.org/10.1016/j.agrformet.2021.108348
Issue Date	2021-05-15
Doc URL	http://hdl.handle.net/2115/89225
Rights	© 2021. This manuscript version is made available under the CC-BY-NC-ND 4.0 license http://creativecommons.org/licenses/by-nc-nd/4.0/
Rights(URL)	http://creativecommons.org/licenses/by-nc-nd/4.0/
Type	article (author version)
File Information	AlbedoRe3_MS.pdf

Title:

Influence of disturbances and environmental changes on albedo in tropical peat ecosystems

Authors:

*Shinjiro Ohkubo[a], Takashi Hirano[a] and Kitso Kusin[b]
*Corresponding author
E-mail: sohkubo@env.agr.hokudai.ac.jp

[a] Research Faculty of Agriculture, Hokkaido University, Sapporo 060-8589, Japan
[b] CIMTROP, University of Palangkaraya, Palangkaraya, 73112, Indonesia

Keywords:

- Deforestation
- Drainage
- Groundwater level
- Haze
- Fire
- Southeast Asia

Abstract

Tropical peat swamp forests have been experiencing drastic disturbances, such as deforestation, drainage, and fire. We examined how such disturbances influence albedo, which regulates radiative energy exchange between the terrestrial surface and the atmosphere. We conducted continuous field observations at three sites: undrained forest (UF), drained forest (DF), and drained burned ex-forest (DB), in Central Kalimantan, Indonesia, for over 13 years.

Observed albedo was strongly influenced by haze caused by fire because the haze layer covering the canopy has a relatively high reflectance. Under severe haze conditions in October 2015, apparent albedo increased to 0.156, 0.162, and 0.183 at the UF, DF, and DB sites respectively. Mean monthly albedos excluding fire periods were 0.094 ± 0.005, 0.092 ± 0.006, and 0.099 ± 0.017 (mean ± 1 standard deviation) at the UF, DF, and DB sites respectively. Seasonal fluctuation in albedo at the DB site, where ferns were dominant, was greater than at the UF and DF sites.

Albedo at the DF site was significantly lower than that at the UF site from February to August ($p < 0.05$). At the forest sites the albedo increased as groundwater level decreased. Albedo was higher under high vapor pressure deficit at all sites. At the DB site albedo decreased when the soil surface was water-saturated and patched with puddles, potentially due to the low albedo of open water. The albedo at the DB site was lower than that at the forest sites at the beginning of the observation period. Subsequently, the albedo increased and exceeded those at the UF and DF sites immediately after fire damage in 2009. This could be explained by the expansion of bright-colored ferns and sedges over dark-colored peat soil. According to our results, haze, groundwater level, and vegetation cover significantly influence albedo in tropical

peat swamp forests.

1. Introduction

Tropical peatlands sequester 105 Gt of soil organic carbon, accounting for 21% of the global peat carbon reserves, and are a major carbon reservoir (Page et al., 2011; Dargie et al., 2017). A significant portion of tropical peat, accounting for approximately 43% of all the tropical peat areas, occurs in Southeast Asia. The environments in numerous tropical peatlands in the region have changed due to the conversion of land, mainly into oil palm and acacia plantations (Miettinen et al., 2016). Drainages is often undertaken to lower the groundwater level (GWL) to facilitate agricultural activities. Consequently, soil aridification occurs, and fire risks increase in the dry season, since dry peat is highly combustible.

The Mega Rice Project (MRP) represents a case where a tropical peatland ecosystem has been degraded (Hoscilo et al., 2011). This project was launched in Central Kalimantan, Indonesia in 1996 to transform a vast peat swamp forest area into farmland, mainly rice fields. However, the MRP was officially canceled in 1999 mainly because of a prevailing economic crisis, leaving behind an abandoned peatland (Rieley and Muhmad, 2002). Consequently, more than 60% of the peat swamp forest in the MRP area disappeared from 1997 to 2000 (Page et al., 2009). In addition, in recent decades, oil palm has attracted the attention of farmers as a profitable cash crop. Consequently, oil palm plantations have expanded rapidly in recent times, especially in Southeast Asia. For example, in Kalimantan, 206,400 ha of peat swamp forest, equivalent to 3.8% of all Kalimantan swamp were converted into oil palm plantations by 2010 (Gunarso et al., 2013).

Numerous studies on tropical peatlands have evaluated the effects of peatland disturbance on carbon dioxide (CO_2) dynamics from a global warming perspective (e.g., Page et al., 2002; Hirano et al., 2012; Itoh et al., 2017; Warren et al., 2017). Drainage of peatlands, which creates aerobic conditions in the environments, stimulates the degradation of peat via microbial activity, which in turn increases CO_2 efflux from the soil to the atmosphere (e.g., Sundari et al., 2012; Hirano et al., 2014; Itoh et al., 2017). Drainage of peatlands also increases fire risk and accelerates fire propagation. Fire is a disturbance that contributes considerably to global warming. In recent decades tropical peatlands in Indonesia, particularly in Sumatra and Kalimantan, repeatedly experienced large-scale fires in El Niño years (1997, 2002, 2009, 2014, and 2015). Huijnen et al. (2016) noted that widespread forest and peatland fires burned over a large area of maritime Southeast Asia in September and October 2015. The CO_2 emission rate (11.3 Tg CO_2 per day) in the region in September–October 2015 exceeded the fossil fuel CO_2 emissions from the European Union (EU28) (8.9 Tg CO_2 per day) for that period. The large-scale fires in the region emitted large amounts of smoke and caused a dense haze which spread out up to the Malay Peninsula and Borneo.

Energy balance between terrestrial surfaces and the atmosphere should be considered, in addition to greenhouse gas fluxes in the evolution of the impact of various disturbances on global warming. Sensible heat, which directly warms the atmosphere, is referred to as net radiation energy. Albedo and incoming solar radiation influence net radiation a great deal. For example, forestation in boreal peatlands caused positive net radiative forcing at one of four sites by decreasing albedo (Lohila et al., 2010), indicating that forestation does not necessarily mitigate global warming. Burakowski et al. (2018) quantified the impact of deforestation on surface temperature in the Eastern United States using on-site data and a model. They reported that surface cooling due to increased albedo that was caused by deforestation was lower than 0.2°C in summer. Zhang et al. (2020) also assessed the contribution of reforestation to global warming by comparing data from six paired forest–grassland sites in temperate zones. They estimated that the albedo warming effect due to reforestation was, on average, 2.3°C. Both studies demonstrated that decreased albedo over forestlands causes surface warming.

Conversely, several studies have also reported that deforestation increases albedo. For example, Loarie et al. (2011) showed that deforestation increased albedo by 2.8% and flooding increased albedo due to the submergence of vegetation in South America. Oliveira et al. (2019) also demonstrated increases in albedo in pasture, agricultural land, and secondary forest following the land conversion from primary tropical forests in southwestern Amazonia. Sabajo et al. (2017) also concluded that albedo in intact forests was lower than in other types of land cover: clear-cut land, palm oil plantation, and rubber plantation in Sumatra. As for peatland, the above-canopy albedo in a burned swamp forest was significantly higher than that of an unburned swamp forest in Finland (Thompson et al., 2015). Kuusinen et al. (2013) reported that the albedo of a clear-cut area was higher than those of forests, excluding that of a birch forest in Finland.

Many studies have evaluated albedo over large areas using satellite products such as MODIS. For example, Li et al. (2015) showed a difference in albedo between forest and open land at the global scale. They revealed that forests have lower albedo than open land, especially in northern mid-latitudes in winter. In the tropical zone (20ºS–20ºN), however, the mean albedo difference between forest and open land was low when compared with differences in the other latitudinal ranges. They also concluded that the cooling or warming effects of forests are mainly driven by evapotranspiration and albedo.

Satellite products are useful in acquiring large-scale data for target areas but there is still room for improvement with regard to precision and resolution. Oliveira et al. (2019) reported that satellite data overestimate albedo as compared to field data. In addition, He et al. (2014) reported that the estimated albedo depends on the type of satellite data employed. Cescatti et al. (2012) analyzed field data obtained from 53 FLUXNET sites and found some mismatch between *in situ* measurements and those from satellite products, especially in grasslands and crop lands, largely due to spatial heterogeneity. Field observations could reveal the characteristics of albedo under different environmental conditions. However, only a few studies based on long-term field observations in tropical peatlands has been conducted (e.g., Hirano et al., 2015; Tang et al., 2019; Kiew et al., 2020). Considering rapidly expanding land conversion, it is very important to evaluate the albedo which would change significantly in tropical peatlands. Albedo affects not only radiation balance directly but also evapotranspiration through energy balance. Evapotranspiration is a key component in water balance and affects GWL, which governs oxidative peat decomposition. Thus, it is important to know how albedo changes following disturbance. In this study we measured meteorological variables, GWL and albedo at three tropical peat ecosystems under different degrees of disturbance, namely undrained forest (UF), drained forest (DF), and drained burned ex-forest (DB) in Central Kalimantan, Indonesia, for more than 13 years. By comparing the albedo responses to environmental variations we examined how the drainage and fire environmental disturbances influenced albedo.

2. Materials and Methods

2.1. Site description

The study area was in the upper catchment of the Sebangau river, approximately 20 km south of Palangkaraya City in Central Kalimantan, Indonesia (Fig. 1). The area was partly within the western section (Block C) of the former Mega Rice Project (MRP). Fire frequently occurred during the dry season and the burnt area increased in size in El Niño periods including 2002–2003, 2004–2005, 2006–2007, 2009–2010, 2012, and 2014–2016, as defined by NOAA (https://www.ncdc.noaa.gov/teleconnections/enso/indicators/sst/). In Central Kalimantan the dry season in normal years lasts for approximately three months, between July and October.

The UF, DF, and DB sites were located within 15 km of each other. UF site was a relatively intact forest, though it had been selectively logged until the late 1990s. DF site had also been selectively logged during the same period, and a large canal was excavated in 1996 and 1997. Although UF and DF sites were evergreen broad-leaved forests, some defoliation was seen, namely not all the leaves were fallen at the end of the dry season (Fig. 2). Hirano et al. (2007) reported that leaf area index (LAI) slightly decreased from October to December. The DB site was burned at least four times; in 1997, 2002, 2009, and 2014. In 2009 sensors and cables on and under the ground were severely damaged by fire. After vegetation was burned in 2009, ferns rapidly grew and covered most of the soil surface. In September 2014 the density of young trees, mainly

Combretocarpus rotundatus (DBH > 3 cm) was 846 trees ha^{-1}. The forest floor was uneven with hummocks and hollows at UF and DF site. Hummocks forming on dense tree roots are generally 20–30 cm higher than surrounding vegetation-free hollows. In contrast, no such microtopography was found in DB site, because hummocks were burned. Further information on the three sites is presented in Table 1 and described by Hirano et al. (2012).

2.2. Measurement

The variables used in the present study are listed in Table 2. Observations were conducted on towers from July 2004 to June 2017 at the UF site, from November 2001 to June 2017 at the DF site, and from April 2004 to February 2017 at the DB site. Some of the data are listed in Table 1.

At the UF and DF sites, downward and upward shortwave radiations were measured using a radiometer (CNR-1; Kipp & Zonen, Delft, the Netherlands) at heights of 36.3 and 40.6 m respectively. At the DB site the height of measurement was elevated twice owing to growth of vegetation (Table 1). Air temperature and relative humidity were measured using a platinum resistance thermometer and a capacitive hygrometer (HMP45; Vaisala, Helsinki, Finland) at heights of 36.3, 41.7, and 1.5 m at the UF, DF, and DB sites respectively, while precipitation was measured using a tipping-bucket rain gauge (TE525; Campbell Scientific Inc., Lorgan, UT, USA) at heights of 36.0, 41.0, and 1.5 m at the UF, DF, and DB sites respectively.

Sensor signals were measured every 10 s and each 30-min average was logged with a datalogger (CR10X or CR1000; Campbell Scientific Inc.). Groundwater level (GWL), defined as the distance between the groundwater surface and the ground surface, was measured half-hourly with a water level logger (DL/N; Sensor Technik Sirnach AG, Sirnach, Switzerland or DCX-22 VG; Keller AG, Winterthur, Switzerland) within 5 m from experimental towers at the three sites. Positive GWLs denote the water levels are aboveground, whereas negative GWLs denote the water levels are belowground. Hirano et al. (2012) provided additional information on measurements.

2.3. Data processing

We defined albedo using the following equation:

$$albedo = S_u \;/\; S_d \tag{1}$$

where S_u is the upward shortwave radiation (W m^{-2}) and S_d is the downward shortwave radiation (W m^{-2}). We used half-hourly data from 10:00 to 14:00 to minimize the effects of solar altitude. Furthermore, data during rain and within an hour after rain events were excluded to eliminate the influence of raindrops on the dome of the radiometer.

As an index for fire scale around the experimental sites, monthly burned fraction (BF) data in each 0.25° grid cell were extracted from the Global Fire Emission Database (https://globalfiredata.org/pages/data/). The cell for the UF site (cell 1) was within 2.25–2.5ºS and 113.75–114ºE and the cells for the DF and DB sites (cell 2) were within 2.25–2.5ºS and 114–114.25ºE. The data were available up until the end of 2016. Albedo chiefly reflects the color and structure of the plant canopy covering the ground surface. The light reflectance of leaves is influenced by leaf moisture and generally increases with a decrease in moisture. We used GWL and vapor pressure deficit (hPa, VPD) as indices of pedospheric and atmospheric dryness. VPD was calculated based on the air temperature and relative humidity data at each site.

We used the aerosol optical depth (AOD) as a reference value for the degree of attenuation of shortwave radiation by haze. AOD was measured with a photometer at a height of 27 m at the Palangkaraya AERONET site (2.23°S, 113.95°E), which is approximately 11 km north of the UF site and approximately 16 km northeast of the DF and DB sites. The observations began on 19 July, 2012. The data were acquired from the AERONET database (https://aeronet.gsfc.nasa.gov/new_web/aerosols.html). We used the highest quality data categorized at level 2.0 (cloud cleared and quality assured).

2.4 Quantitative evaluation of the haze effect on albedo

Frequent fires in the dry season cause haze and affect the atmospheric optical environment, namely through transmission, scattering, and absorption of shortwave radiation. We examined the haze effect quantitatively by calculating the increases or decreases from the values under no-haze conditions. The haze layer between the observation height (H_{obs}) and canopy height (H_{cano}) was used for calculations. We also examined the validity of our directly measured albedo with radiometers by comparing observed albedo and theoretically calculated albedo at the observation heights. To do this (refer to Fig. 3), we defined the reflectance, absorbance, and transmittance of the haze layer as β, γ, and λ ($\beta + \gamma + \lambda = 1$). Incoming S_d at H_{obs} is distributed into reflected upward radiation at H_{obs} (βS_d), absorbed radiation in the layer (γS_d), and transmitted radiation to H_{cano} (λS_d). Defining albedo at the canopy as α_{cano}, λS_d was reflected upward as $\alpha_{cano}\lambda S_d$, and then attenuated through the haze layer and reached H_{obs} as $\alpha_{cano}\lambda^2 S_d$. Therefore, S_u and albedo at H_{obs} (α_{obs}) are expressed as follows:

$$S_u = \alpha_{cano}\lambda^2 S_d + \beta S_d \tag{2}$$

$$\alpha_{obs} = \frac{S_u}{S_d} = \frac{\alpha_{cano}\lambda^2 S_d + \beta S_d}{S_d} = \alpha_{cano}\lambda^2 + \beta \tag{3}$$

Note that $\lambda \approx 1$ and $\beta \approx 0$ under no haze conditions because the distance between H_{obs} and H_{cano} was relatively short (less than 15 m).

The transmittance λ was calculated using the Beer-Lambert Law, as follows:

$$\lambda = \exp\left(-b_{ext}x_L\right) \tag{4}$$

where x_L is the distance between H_{obs} and H_{cano}, and b_{ext} is the extinction coefficient. According to the results of laboratory experiments under daylight viewing conditions, λ=0.02 is usually employed as the perceptible threshold for visual range calculations (Seinfeld and Pandis, 2006). When λ=0.02, the visibility distance x_v can be evaluated using the following equation (the Koschmeider equation):

$$x_v = \frac{3.912}{b_{ext}} \tag{5}$$

To facilitate the comparison of the results of the present study with those of previous studies we performed calculations under the most severe haze conditions with AOD = 3 for the DF site. According to Kusumaningtyas et al. (2016) x_v is shorter than 500 m at an AOD of 3. Therefore, b_{ext} is calculated to be more than 7.82×10^{-3} m^{-1}. In addition, applying the distance x_L=14.6 m between H_{obs}=40.6 m and H_{cano}=26 m at the DF site in Eq. 4, λ is calculated to be lower than 0.89, which indicates that $\beta+\gamma$ is greater than 0.11 (1 – 0.89 = 0.11). According to Seinfeld and Pandis (2006), light scattering by particles with sizes comparable to the wavelength of visible light is largely responsible for visibility reduction in the atmosphere and scattering by particles accounts for 50–95% of light extinction. In non-urban sites scattering and absorption account for 80–95% and 10–25% light extinction respectively. Assuming that backscattering radiation to the atmosphere (βS_d) is 80% of the extinction of S_d (β / ($\beta + \gamma$) = 0.80), β is calculated as 0.086. The above equations and calculations will be used in the Discussion section.

3. Results

3.1 Overview of meteorological conditions

Figure 4 presents a time series of monthly environmental variables from 2004 to 2017. Monthly precipitation ranged from 80, 82, and 82 mm in August to 341, 323, and 326 mm in December on average in 2004–2016 at the UF, DF, and DB sites respectively. Similar seasonal variations in precipitation were seen at the all three sites, in which precipitation started to decrease in May until August then started to increase in September until November. Mean annual precipitation from 2005 to 2016 was 2663 ± 479, 2623 ± 479, and 2641 ± 473 mm (mean ± 1 standard deviation) at the UF, DF, and DB sites respectively. Meanwhile, annual air temperature exhibited slight seasonal fluctuation with bimodal peaks in May and October. Mean annual air temperatures from 2005 to 2016 were 26.1 ± 0.5, 26.1 ± 0.2, and 26.4 ± 0.3 °C at the UF, DF, and DB sites respectively. Variation in the GWL was synchronized with precipitation events. In the wet season, GWL became positive (aboveground) at the UF and DB sites whereas it remained negative (belowground) at the DF site. GWL at the DB site has decreased since 2014 due to the drainage channel excavation activities nearby.

Albedos at the UF and DF sites had been increasing slightly with occasional rises. Conversely, albedo at the DB site increased gradually, with seasonal fluctuation throughout the observation period. Monthly BF data in the two cells were almost synchronized, although cell 2 had a higher BF than cell 1. BF in cell 2 was the highest, at 0.10, in September 2009, when the DB site was damaged severely by fire.

3.2 Seasonal variation in albedo

Figure 5 shows the monthly ensemble average of albedo at the three sites. Data plots were classified using BF. Albedo generally increased with an increase in BF in the dry season. Excluding the influence of haze (BF ≥ 0.005), monthly averages ranged from 0.092 in May to 0.096 in December at the UF site, from 0.087 in April to 0.098 in December at the DF site, and from 0.087 in April to 0.109 in September at the DB site. The mean monthly albedo with BF<0.005 over the entire observation period was 0.094 ± 0.005, 0.092 ± 0.006, and 0.099 ± 0.017 (mean ± 1 standard deviation) at the UF, DF, and DB sites respectively, excluding the data during fires. There were significant differences (p<0.01) of albedo at DB site with those at UF and DF sites from the whole study period. Figure 6 illustrates the inter-site differences in monthly albedo with 95% confidence intervals determined using the bootstrap method with 1000 repetitions. From February to August, the albedo at the DF site was significantly lower than that at the UF site (p<0.05). Albedo at the DB site was significantly greater (p<0.05) than the albedo at the UF site in July, September, and October, and that at the DF site from July to October. All monthly albedo values at each site are listed in the Appendix.

3.3 Inter-annual variation in albedo

Albedo at the DB site increased annually since observations began (Fig. 4c). At the end of 2016 the albedo recorded was 0.131, exceeding those at the UF and DF sites by more than 0.02. Figure 7 illustrates the inter-annual variation in albedo at the three sites. Annual increments in albedo were calculated by applying linear regression to the data only in April–June to eliminate the influence of fire and to use the entire datasets at all the sites. BF in April–June was below 0.005 throughout the observation period (Fig. 7). The increasing rate at the DB site was the highest (0.0044 year^{-1}, R^2 = 0.76, p < 0.01), followed by the DF site (0.0013 year^{-1}, $R^2 = 0.74$, $p < 0.01$) and UF site (0.0007 year^{-1}, $R^2 = 0.50$, $p < 0.01$).

3.4 Influence of environmental conditions

Generally, the timing of positive peaks of albedo in the dry season corresponded to negative peaks of GWL and positive peaks of BF and AOD, especially in 2006, 2009, and 2015 (Fig. 4b–e). In 2015 the maximum albedo levels were 0.156, 0.162, and 0.183 at the UF, DF, and DB sites, respectively. In addition, BF had positive peaks of 0.042 in cell 1 and 0.087 in cell 2, and AOD reached 3.79. In contrast, although BF and AOD had their positive spikes in 2012, no clear sharp spikes of albedo were observed.

The influence of water conditions on light reflection characteristics was examined. The relationship between albedo and GWL is illustrated in Figure 8. Daily average data were classified by AOD. High albedo (below around −1.0 m) was observed at low GWL ranges at all sites. Generally, albedo increased with an increase in AOD. Some plots with AOD ≥ 0.5 were also observed at relatively high GWLs from September to October 2012, during which time GWL did not decrease markedly, while AOD peaked (Fig. 4). Excluding the AOD ≥ 0.5 data, albedo showed a significant negative relationship with GWL at the UF and DF sites. Conversely, the albedo at the DB site was not significantly correlated with GWL when GWL < 0 m. When groundwater rose aboveground (GWL ≥ 0 m), albedo seemed to be lower than the estimated value by the fitted line for GWL<0 at the DB site but not at the UF site.

Figure 9 illustrates the relationship between albedo and VPD. Data with AOD ≥ 1.0 were generally greater than data with AOD < 0.5. Albedo increased slightly at the lowest and highest VPD ranges (VPD<ca.10 and VPD≥ca.25 hPa) at the UF and DF

sites. For the AOD < 0.5 data, the quadratic relationships were significant ($p < 0.05$). On the other hand, linear and quadratic fittings were roughly overlapped each other and both fitting lines showed increasing trend of albedo with VPD within the observed range at DB site.

4. Discussion

4.1 Comparison with other studies

Table 3 provides a range of literature values from this study and previous studies. The mean observed albedo values (0.092–0.099) at BF < 0.005 at the sites were lower than those in other tropical forests: 0.114–0.12 in an Amazonia forest (Cescatti et al., 2012; Oliveira et al., 2019). Peat swamp forests might have canopy structures similar to those of Amazonian forests, forming dense crown canopies of evergreen broadleaf trees. However, in our study area a few small canopy gaps were generated by tree fall especially at the DF site. The reduction in upward reflection due to the resulting uneven canopy could be the reason for the lower albedo at our forest sites. In addition, the albedo observed in the present study was much lower than that in treeless peatlands: 0.132 at a Finnish peat bog in summer (Gao et al., 2014); 0.137 at an open mesotrophic fen on a Finnish peat soil in July (Lohila et al., 2010); and 0.140 at an open Finnish peatland in summer (Kuusinen et al., 2013). Bright-colored short vegetation dominating the ground surface could be the reason for the higher albedo in treeless peatlands.

4.2 Influence of land cover change

Compared with that at the forest sites (UF and DF), albedo at the burned site (DB) was higher after a severe fire in 2009, when the ground was mostly covered with vegetation mainly comprising ferns (Fig. 4c). Many studies have reported an increasing albedo following deforestation in the tropics. For example, albedo increased by 0.027 and 0.032 following the conversion of tropical forests into pasture and agricultural land respectively in southwestern Amazonia (Oliveira et al., 2019). Berbet and Costa (2003) reported that the albedo increased by 0.043 following the replacement of a tropical forest with pasture in Amazonia. In addition, Sabajo et al. (2017) reported that the albedo of clear-cut areas was 0.02 higher than that of forests in Sumatra, Indonesia. However, the albedo of the DB site was lower than those of the UF and DF sites until the middle of 2009 (Fig. 4c), potentially because relatively dark colored bare peat was still largely exposed. In contrast, Thompson et al. (2015) reported that albedo at a burned peat bog was higher than that at an unburned site over a two-year period following a wildfire, with no clear difference detected after four years. They explained that the higher albedo at the burned site was due to the immediate recovery of *Sphagnum* moss over the peat soil.

The albedo of the DB site exhibited an increasing trend up to 0.131 at an annual rate of 0.0044 year^{-1} until 2016 (Fig. 7c). An increase in albedo after fire, which represented a 0.08 increase over the first decade, was also observed in burned boreal forests (Amiro et al., 2006). The albedo of 0.131 was generally lower than that observed in shrubland, savanna, grassland, and cropland (e.g., Myhre et al., 2005; He et al., 2018; Ge et al., 2019). The comparison of albedo at DB site with those at reference sites mentioned above and Figure 7c suggest that albedo continued to increase at the DB site as long as the existing light-colored herbaceous plants was expanding. Page et al. (2009) reported that a high-intensity fire prevents transition of non-forest vegetation or bare peat into forest and replaces the plant community with ferns and sedges with few or no trees. Over the last few decades, fire has occurred so frequently that DB sites have become dominated by ferns and no change in this condition is expected. Therefore, observations at short term intervals are essential to capture such dynamic variation and to make precise estimates of albedo.

The annual albedo of forest sites has also been increasing gradually (Fig. 7), although the annual rates of 0.0007 year^{-1} at the UF site and 0.0013 year^{-1} at the DF site were lower than 30% of the rate observed at the DB site. Increasing albedo could reflect subtle changes in canopy structure with gradual tree growth. For example, canopy gaps were changing following the termination of selective logging in the late 1990s. Tree growth resulting in filling of canopy gaps would smooth the forest canopy and thus, increase albedo. Canopy recovery after tower construction might be another reason for the inter-annual increase.

4.3 Seasonal variation in albedo

The larger seasonal fluctuation in albedo observed at the DB site as compared with the fluctuations at the UF and DF sites (Figs. 4 and 5) could be due to the greater seasonal fluctuation in ground conditions at the DB site, including exposure of peat soil and growth of ferns. The bare ground at the DB site, was much more exposed due to sparsely distributed vegetation. Basically, peat soil turns dark in the wet season and light in the dry season, depending on the GWL. At the UF and DF sites, however, the ground surface was almost entirely covered by a dense canopy. In addition, ferns dominating the DB site lightened leaf color in the dry season because of the decrease of leaf water content. Therefore, the albedo at the DB site increased in the dry season.

The annual amplitudes of albedo at the forest sites (0.004 at the UF site and 0.011 at the DF site, on average) were lower than those at other tropical forests (0.025; Berbet and Costa, 2003). The larger annual amplitudes were due to decreasing LAI in the dry period, resulting in higher albedo. Myneni et al. (2007) reported that the Amazon rainforest exhibits notable LAI seasonality with an annual amplitude of 25%. Our smaller annual range would indicate weaker LAI phenology.

4.4 Influence of fire smoke

The AOD was similar in magnitude and seasonal variation to those in Amazonian forests. Oliveira et al. (2007) reported that AOD exceeded 3.0 during the dry season due to biomass burning events. Schafer et al. (2008) showed that AOD at 440 nm peaked in the dry season when fire occurred. Generally, AOD is a reliable index for fire smoke.

To examine the reliability of the albedo data measured directly with radiometers under the most severe haze conditions in the present study with an AOD of 3 at the DF site, we calculated α_{obs} using Eq. 3 for comparison with the observed α_{obs}. By assuming $\alpha_{obs} \approx \alpha_{cano}$ at BF<0.005 and applying the mean albedo (0.092) for α_{cano} with β = 0.086 and λ= 0.89 to Eq. 3, α_{obs} was calculated to be 0.160. This value was comparable to the observed values (0.14 ± 0.02, mean ± 1 standard deviation) at AOD $\geq$ 3 in Figs. 8b and 9b; α_{obs} is 174 % of α_{cano}. That is, 74 % of overestimation was caused by haze. When x_v is a half (250 m) or double (1000 m) the distance of 500 m, α_{obs} is calculated to be 0.221 and 0.126, respectively. Similarly, when x_L is a half (7.3 m) or double (29.2 m) the actual distance (14.6 m), α_{obs} is calculated to be 0.126 and 0.221 respectively, with x_{v} = 500 m.

The calculated values above clearly indicate that severe haze causes the overestimation of surface albedo and that albedo strongly depends on the distance between the observation height and the vegetation height. Therefore, distinctly high albedo during fire events must have resulted from the haze layers below the radiometer and not from sharp responses of vegetation. It is quite challenging to determine canopy albedo using single-point observations above the canopy under severe haze conditions. The degree of the haze effect on albedo was quantitatively demonstrated using equations 2 and 3.

4.5 The response of albedo to GWL and VPD

First, we explain the variation in GWL at the DB site because GWL remained high until 2014 despite the drainage. The high GWL was partly caused by ground lowering due to the loss of surface peat by repeated fires. For example, surface peat was burned by 0.22 m in thickness in 2002 at DB site (Hirano et al., 2014). Another reason for the high GWL would be lower evapotranspiration due to low tree density (Hirano et al., 2015). However, GWL has decreased since 2014 because of channel excavation nearby.

Albedo clearly decreased at the DB site when GWL was positive (Fig. 8). Generally, the albedo of open water is lower than that of soil. Thus, the appearance of open water on the ground surface at the DB site, where some small puddles were exposed to the sky in the wet season, could have contributed to the decrease in albedo. In contrast, such a decrease in albedo was not observed even during flooding at the UF site because the soil surface was mostly covered with canopy. Loarie et al. (2011) reported a similar result, where flooding decreased forest albedo in South America.

In the forest sites in the present study, defoliation increased slightly in October–December (data not shown). In addition negative GWL peaks were regularly observed in September–October. Leaf color turns brighter due to drying during the dry season with a slight corresponding decrease in LAI. Therefore, albedo had a negative relationship with GWL (Fig. 8) at the UF and DF sites. Sanchez-Mejia et al. (2014) have also investigated the relationship between albedo and GWL in a semiarid shrubland. They reported that albedo increased by about 0.03 in a closed canopy site and by about 0.05 in an open site with a lowering of GWL 0 to −0.6 m. The rates of increase are higher than those observed at our sites: 0.006 (UF), 0.005 (DF), and 0.001 (DB), following the lowering of GWL by 0.6 m (Fig. 8).

An increase in albedo with a lowering of GWL seems to be inconsistent as in this study in which the albedo at the DF site was not greater than that at the UF site. Although the differences between the UF and DF sites in canopy structure, tree species and phenology are potential reasons for the discrepancy, further investigations are required to establish robust evidence to explain this inconsistency.

In the present study the albedo increased at the lowest VPD range (VPD<ca.10 hPa) at the UF and DF sites. Water droplet might increase reflection of incoming solar radiation. Some water droplets might have remained on the leaf surfaces at the UF and DF sites even more than an hour after the rainfall under low VPD conditions whereas water droplets easily evaporated at the DB site. This could be because of the difference in vegetation height and structure between the forest and burned sites. Conversely, albedo increased at the highest VPD range (VPD≥ca.25 hPa) at all three sites, potentially because leaf surfaces become lighter and reflection on leaf surfaces is enhanced to facilitate adaptation to water deficit under dry atmospheric conditions (e.g., Yu et al., 2000). Therefore, changes in pedospheric and atmospheric moisture (or dryness) influenced albedo via vegetation responses, especially those of leaves.

5. Conclusions

Our continuous long-term field observations revealed the impact of fire and water conditions (GWL and VPD) on albedo in tropical peat ecosystems. Fire decreased land surface albedo by exposing the dark-colored peat soil. Subsequently, ferns regenerated immediately and expanded over the ground surface. Conversely, intensive fire sometimes caused severe haze. Apparent albedo sharply increased under such hazy conditions because the haze layer between the radiometer and canopy increased reflection of incoming downward radiation. Hence, the albedo of vegetation cannot be measured under such hazy conditions. Nevertheless, decreasing GWL slightly increased the albedo in both the undrained and drained forests. At the highest VPD range (VPD≥ca.25 hPa), the albedo increased at all sites. Therefore, both pedospheric and atmospheric dryness increased albedo. When the soil surface was water-saturated (GWL ≥ 0 m), albedo at the burned site decreased because the ground was dotted with exposed puddles. In contrast, no decrease was observed in the undrained forest because open water with low albedo was covered by the forest canopy.

We observed several environmental changes in response to rapidly shifting land surface characteristics. Therefore, short-interval measurements are required for the accurate evaluation of change in albedo. Our study also explored changes in albedo under heterogeneous environments. The expansion of the target area to the entire Southeast Asia and observation of trends under diverse meteorological conditions over different land cover types, including oil palm and acacia plantations, would be insightful. In addition, long-term continuous field observations before and after land conversion would reveal impacts with a high temporal resolution.

Acknowledgements

This study was supported by JSPS Core University Program, JSPS KAKENHI Grant Numbers 13375011, 1525001, 21255001, 25257401, and 19H05666, the JST-JICA Project (SATREPS) (Wild Fire and Carbon Management in Peat-Forest in Indonesia) and Technology Development Fund (no. 2-1504) by the Environmental Restoration and Conservation Agency and the Ministry of the Environment, Japan. We are grateful to the late Dr. Suwido Limin for the site establishment. We also express our gratitude to the providers of burned fraction datasets of GFED, and Drs. Herizal, Catur Winarti, and Davis Setyo Nugroho for their efforts in establishing and maintaining the Palangkaraya AERONET site and for provision of data.

References

Amiro, B.D., Orchansky, A.L., Barr, A.G., Black, T.A., Chambers, S.D., Chapin, F.S., Goulden, M.L., Litvak, M., Liu, H.P., McCaughey, J.H., McMillan, A., Randerson, J.T., 2006. The effect of post-fire stand age on the boreal forest energy balance. Agric. For. Meteorol. 140, 41–50. https://doi.org/10.1016/j.agrformet.2006.02.014.

Berbet, M.L.C., Costa, M.H., 2003. Climate change after tropical deforestation: seasonal variability of surface albedo and its effects on precipitation change. J. Clim. 16, 2099–2104. https://doi.org/10.1175/1520-0442(2003)016<2099:CCATDS>2.0.CO;2.

Burakowski, E., Tawfik, A., Ouimette, A., Lepine, L., Novick, K., Ollinger, S., Zarzycki, C., Bonan, G., 2018. The role of surface roughness, albedo, and Bowen ratio on ecosystem energy balance in the Eastern United States. Agric. For. Meteorol. 249, 367–376. https://doi.org/10.1016/j.agrformet.2017.11.030.

Cescatti, A., Marcolla, B., Vannan, S.K.S., Pan, J.Y., Román, M.O., Yang, X., Ciais, P., Cook, R.B., Law, B.E., Matteucci, G., Migliavacca, M., Moors, E., Richardson, A.D., Seufert, G., Schaaf, C.B., 2012. Intercomparison of MODIS albedo retrievals and in situ measurements across the global FLUXNET network. Remote Sens. Environ. 121, 323–334. https://doi.org/10.1016/j.rse.2012.02.019.

Dargie, G.C., Lewis, S.L., Lawson, I.T., Mitchard, E.T.A., Page, S.E., Bocko, Y.E., Ifo, S.A., 2017. Age, extent and carbon storage of the central Congo Basin peatland complex. Nature 542, 86–90. https://doi.org/10.1038/nature21048.

Gao, Y., Markkanen, T., Backman, L., Henttonen, H.M., Pietikäinen, J.P., Mäkelä, H.M., Laaksonen, A., 2014. Biogeophysical impacts of peatland forestation on regional climate changes in Finland. Biogeosciences 11, 7251–7267. https://doi.org/10.5194/bg-11-7251-2014.

Ge, J., Pitman, A.J., Guo, W., Wang, S., Fu, C., 2019. Do uncertainties in the reconstruction of land cover affect the simulation of air temperature and rainfall in the CORDEX region of East Asia? J. Geophys. Res. Atmos. 124, 3647–3670. https://doi.org/10.1029/2018JD029945.

Gunarso, P., Hartoyo, M.E., Agus, F., Killeen, T.J., 2013. Oil palm and land use change in Indonesia, Malaysia and Papua New Guinea. Reports from the Technical Panels of the 2nd Greenhouse Gas Working Group of the Roundtable on Sustainable Palm Oil (RSPO) 29–64.

He, T., Liang, S., Song, D.X., 2014. Analysis of global land surface albedo climatology and spatial-temporal variation during 1981–2010 from multiple satellite products. J. Geophys. Res. Atmos. 119, 10,281–10,298. https://doi.org/10.1002/2014JD021667.

He, T., Liang, S., Wang, D., Cao, Y., Gao, F., Yu, Y., Feng, M., 2018. Evaluating land surface albedo estimation from Landsat MSS, TM, ETM+, and OLI data based on the unified direct estimation approach. Remote Sens. Environ. 204, 181–196. https://doi.org/10.1016/j.rse.2017.10.031.

Hirano, T., Segah, H., Kusin, K., Limin, S., Takahashi, H., Osaki, M., 2012. Effects of disturbances on the carbon balance of tropical peat swamp forests. Global Change Biol. 18, 3410–3422. https://doi.org/10.1111/j.1365-2486.2012.02793.x.

Hirano, T., Kusin, K., Limin, S., Osaki, M., 2014. Carbon dioxide emissions through oxidative peat decomposition on a burnt tropical peatland. Global Change Biol. 20, 555–565. https://doi.org/10.1111/gcb.12296.

Hirano, T., Kusin, K., Limin, S., Osaki, M., 2015. Evapotranspiration of tropical peat swamp forests. Global Change Biol. 21, 1914–1927. https://doi.org/10.1111/gcb.12653.

Hoscilo, A., Page, S.E., Tansey, K.J., Rieley, J.O., 2011. Effect of repeated fires on land-cover change on peatland in southern Central Kalimantan, Indonesia, from 1973 to 2005. Int. J. Wildland Fire 20, 578–588. https://doi.org/10.1071/WF10029.

Huijnen, V., Wooster, M. J., Kaiser, J. W., Gaveau, D. L. A., Flemming, J., Parrington, M., Inness, A., Murdiyarso, D., Main, B., Weele, M., 2016. Fire carbon emissions over maritime Southeast Asia in 2015 largest since 1997. Sci. Rep. 6, 26,886. https://doi.org/10.1038/srep26886.

Itoh, M., Okimoto, Y., Hirano, T., Kusin, K., 2017. Factors affecting oxidative peat decomposition due to land use in tropical peat swamp forests in Indonesia. Sci. Total Environ. 609, 906–915. https://doi.org/10.1016/j.scitotenv.2017.07.132.

Kiew, K., Hirata, R., Hirano, T., Xhuan, W.G., Aries, E.B., Kemudang, K., Wenceslausa, J., San, L.K., Melling, L., 2020. Carbon dioxide balance of an oil palm plantation established on tropical peat. Agric. For. Meteorol. 295, 108189. https://doi.org/10.1016/j.agrformet.2020.108189

Kusumaningtyas, S.D.A., Aldrian, E., Rahman, M.A., Sopaheluwakan, A., 2016. Aerosol properties in central Kalimantan due to peatland fire. Aerosol Air Qual. Res. 16, 2757–2767. https://doi.org/10.4209/aaqr.2015.07.0451.

Kuusinen, N., Tomppo, E., Bermimger, F., 2013. Linear unmixing of MODIS albedo composites to infer subpixel land cover type albedos. Int. J. Appl. Earth Obs. 23, 324–333. https://doi.org/10.1016/j.jag.2012.10.005.

Li, Y., Zhao, M., Motesharrei, S., Mu, Q., Kalnay, E., Li, S., 2015. Local cooling and warming effects of forests based on satellite observations, Nat. Commun. 6, 6603. https://doi.org/10.1038/ncomms7603.

Loarie, S.R., Lobell, D.B., Asner, G.P., Field, C.B., 2011. Land-Cover and Surface Water Change Drive Large Albedo Increases in South America, Earth Interact. 15, 1–16. https://doi.org/10.1175/2010EI342.1.

Lohila, A., Minkkinen, K., Laine, J., Savolainen, I., Tuovinen, J.P., Korhonen, L., Laurila, T., Tietäväinen, H., Laaksonen, A., 2010. Forestation of boreal peatlands: impacts of changing albedo and greenhouse gas fluxes on radiative forcing. J. Geophys. Res. 115, G04011, https://doi.org/10.1029/2010JG001327.

Miettinen, J., Shi, C., Liew, S.C., 2016. Land cover distribution in the peatlands of Peninsular Malaysia, Sumatra and Borneo in 2015 with changes since 1990. Glob. Ecol. Conserv. 6, 67-78. https://doi.org/10.1016/j.gecco.2016.02.004.

Myhre, G., Kvalevag, M., Schaaf, C.B., 2005. Radiative forcing due to anthropogenic vegetation change based on MODIS surface albedo data, Geophys. Res. Lett. 32, L21410. https://doi.org/10.1029/2005GL024004.

Myneni, R.B., Yang, W., Nemani, R.R., Huete, A.R., Dickinson, R.E., Knyazikhin, Y., Didan, K., Fu, R., Juárez, R.I.N., Saatchi, S.S., 2007. Large seasonal swings in leaf area of Amazon rainforests. Proc. Natl. Acad. Sci. U.S.A. 104 (12), 4820–4823. https://doi.org/10.1073/pnas.0611338104.

Oliveira, P.H.F., Artaxo, P., Pires, C., Lucca, S., Procopio, A., Holben, B., Schafer, J., Cardoso, L.F., Wofsy, S.C., Rocha, H.R., 2007. The effects of biomass burning aerosols and clouds on the CO_2 flux in Amazonia. Tellus B 59, 338–349. https://doi.org/10.1111/j.1600-0889.2007.00270.x.

Oliveira, G., Brunsell, N.A., Moraes, E.C., Shimabukuro, Y.E., Santos, T.V., Randow, C., Aguiar, R.G., Aragao, L.E.O.C., 2019. Effects of land-cover changes on the partitioning of surface energy and water fluxes in Amazonia using high-resolution satellite imagery. Ecohydrology 12, e2126. https://doi.org/10.1002/eco.2126.

Page, S., Hoscilo, A., Wösten, H., Jauhiainen, J., Silvius, M., Rieley, J., Ritzema, H., Tansey, K., Graham, L., Vasander, H., Limin, S., 2009. Restoration ecology of lowland tropical peatlands in Southeast Asia: current knowledge and future research directions. Ecosystems 12, 888–905. https://doi.org/10.1007/s10021-008-9216-2.

Page, S.E., Siegert, F., Rieley, J.O., Boehm, H.D.O., Jaya, A., Limin, S., 2002. The amount of carbon released from peat and forest fires in Indonesia during 1997. Nature 420, 61–65. https://doi.org/10.1038/nature01131.

Page, S.E., Rieley, J.O., Banks, C.J., 2011. Global and regional importance of the tropical peatland carbon pool. Global Change Biol. 17, 798–818. https://doi.org/10.1111/j.1365-2486.2010.02279.x.

Rieley, J., Muhamad, N.Z., 2002. Impact of inappropriate land use change on the peat swamps of Central Kalimantan. Peatlands International 1, 24–27.

Sabajo, C.R., Maire, G., June, T., Meijide1, A., Roupsard, O., Knohl, A., 2017. Expansion of oil palm and other cash crops causes an increase of the land surface temperature in the Jambi province in Indonesia. Biogeosciences 14, 4619–4635. https://doi.org/10.5194/bg-14-4619-2017.

Sanchez-Mejia, Z.M., Papuga, S.A., Swetish, J.B., van Leeuwen, W.J.D., Szutu, D., Hartfield, K., 2014. Quantifying the influence of deep soil moisture on ecosystem albedo: The role of vegetation, Water Resour. Res. 50, 4038–4053. https://doi.org/10.1002/2013WR014150.

Schafer, J.S., Eck, T.F., Holben, B.N., Artaxo, P., Duarte, A.F., 2008. Characterization of the optical properties of atmospheric aerosols in Amazônia from long-term AERONET monitoring (1993–1995 and 1999–2006). J. Geophys. Res. 113, D04204, https://doi.org/10.1029/2007JD009319.

Seinfeld, J.H., Pandis, S.N. 2006. Atmospheric Chemistry and Physics: From Air Pollution to Climate Change. 2nd Edition, John Wiley & Sons, New York.

Sundari, S., Hirano, T., Yamada, H., Kusin, K., Limin, S., 2012. Effects of groundwater level on soil respiration in tropical peat swamp forests. J. Agric. Meteorol. 68, 121–134. https://doi.org/10.2480/agrmet.68.2.6.

Tang, A.C.I., Stoy, P.C., Hirata, R., Musin, K.K., Aries, E.B., Wenceslausa, J., Shimizu, M., Melling, L., 2019. The exchange of water and energy between a tropical peat forest and the atmosphere: Seasonal trends and comparison against other tropical rainforests. Sci. Total Environ. 683, 166–174. https://doi.org/10.1016/j.scitotenv.2019.05.217.

Thompson, D.K., Baisley, A.S., Waddington, J.M., 2015. Seasonal variation in albedo and radiation exchange between a burned and unburned forested peatland: implications for peatland evaporation. Hydrol. Processes 29, 3227–3235. https://doi.org/10.1002/hyp.10436.

Warren, M., Frolking, S., Dai, Z., Kurnianto, S., 2017. Impacts of land use, restoration, and climate change on tropical peat carbon stocks in the twenty-first century: implications for climate mitigation. Mitig. Adapt. Strat. Gl. 22, 1041–1061. https://doi.org/10.1007/s11027-016-9712-1.

Yu, G-R., Miwa, K., Nakayama, K., Matsuoka, N., Kon, H., 2000. A proposal for universal formulas for estimating leaf water status of herbaceous and woody plants based on spectral reflectance properties. Plant and Soil 227, 47–58. https://doi.org/10.1023/A:1026556613082.

Zhang, Q., Barnes, M., Benson, M., Burakowski, E., Oishi, A.C., Ouimette, A., Sanders-DeMott, R., Stoy, P.C., Wenzel, M., Xiong, L., Yi, K., Novick, K.A., 2020. Reforestation and surface cooling in temperate zones: mechanisms and implications. Global Change Biol. 26, 3384–3401. https://doi.org/10.1111/gcb.15069.

Figure legends

Fig. 1 Map of the study area.

Fig. 2 Canopy photos of (a) UF, (b) DF and (c, d) DB sites.

Fig. 3 Schematic diagram of the partitioning of incoming shortwave radiation under severe haze conditions.

Fig. 4 Monthly variations in (a) precipitation, (b) GWL, (c) albedo, (d) BF, and (e) AOD. Precipitation shown in panel (a) was observed at the DF site. Month with BF > 0.02 in either cell was shown by shading in panel (b)-(e) as indicating fire event. Beginning month of canal construction in the vicinity of DB site is marked with an arrow in panel (b).

Fig. 5 Seasonal variations in monthly mean albedo at (a) UF, (b) DF, and (c) DB sites. Plots are classified into five categories by BF: BF<0.005, 0.005≤BF<0.01, 0.01≤BF<0.02, 0.02<BF≤0.03, and 0.03≤BF. The polyline connects the monthly average with BF<0.005. Grey bars show the 95% confidence interval determined by a bootstrap method with 1000 replications.

Fig. 6 Inter-site differences in monthly albedo. The mean (plots) and 95% confidence interval (bars) were determined by the bootstrap method with 1000 replications.

Fig. 7 Inter-annual variation in albedo at (a) UF, (b) DF, and (c) DB sites. Monthly data for only April–June are shown to exclude the influence of fire.

Fig. 8 Relationship between albedo and GWL at (a) UF, (b) DF, and (c) DB sites. Plots were classified into five categories by AOD: AOD<0.5, 0.5≤AOD<1, 1≤ AOD<2, 2≤AOD<3, and 3≤AOD. Data with AOD ≥ 0.5 in September–October 2012 were marked with crosses. A line was fitted to the data with AOD<0.5. In panel (c), line fitting was separately applied to two GWL ranges: GWL<0 and GWL≥0.

Fig. 9 Relationship between albedo and VPD at (a) UF, (b) DF, and (c) DB sites. Plots are classified into five categories by AOD, as shown in Fig. 8.

Figure 1

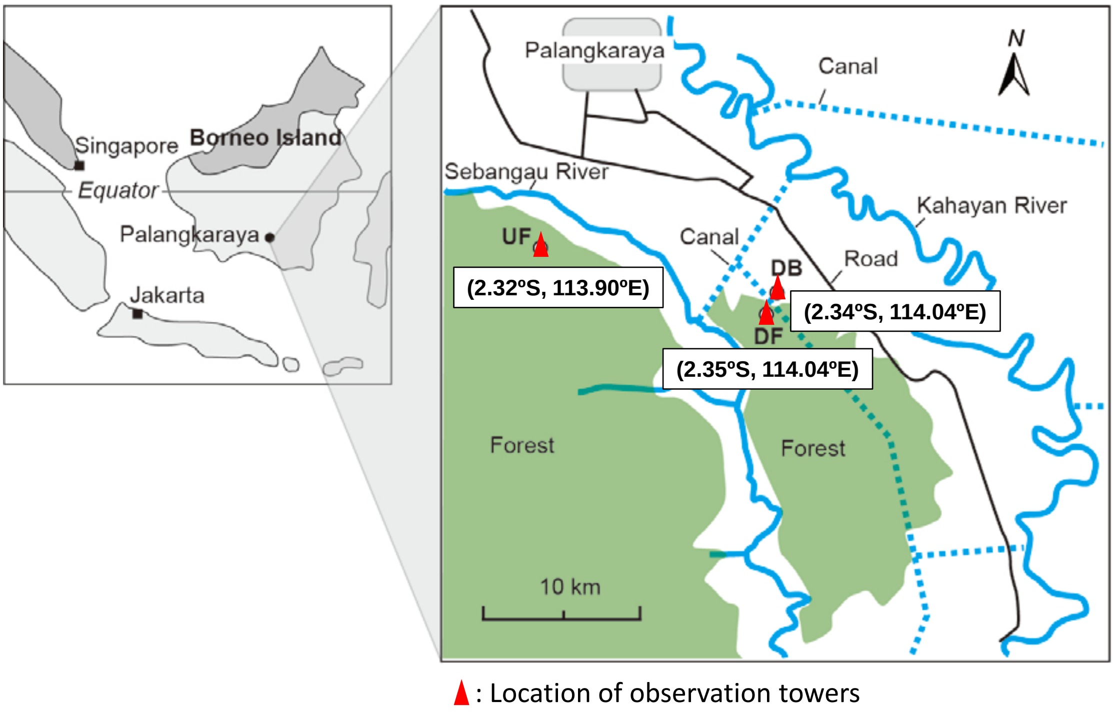
Singapore
Borneo Island
Equator
Palangkaraya
Jakarta
Palangkaraya
Canal
N
Sebangau River
Kahayan River
Canal
Road
UF
(2.32ºS, 113.90ºE)
DB
(2.34ºS, 114.04ºE)
DF
(2.35ºS, 114.04ºE)
Forest
Forest
10 km
▲: Location of observation towers

Figure 2

(a) UF site

(b) DF site

(c) DB site in a dry condition

(d) DB site in a wet condition

Figure 3

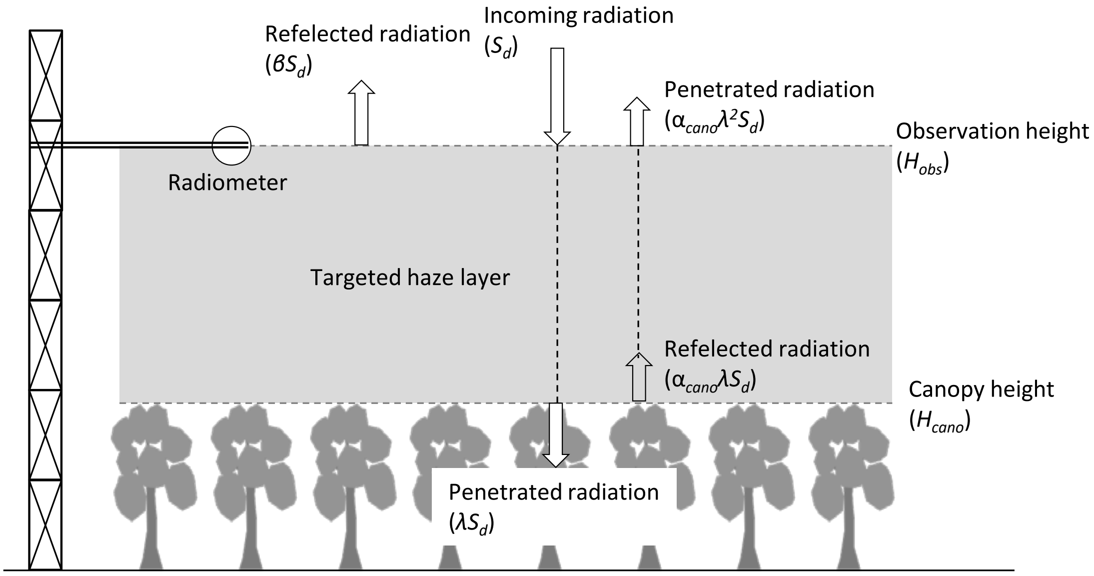
Refelected radiation (βS_d)
Incoming radiation (S_d)
Penetrated radiation ($\alpha_{cano}\lambda^2 S_d$)
Observation height (H_{obs})
Radiometer
Targeted haze layer
Refelected radiation ($\alpha_{cano}\lambda S_d$)
Canopy height (H_{cano})
Penetrated radiation (λS_d)

Figure 4

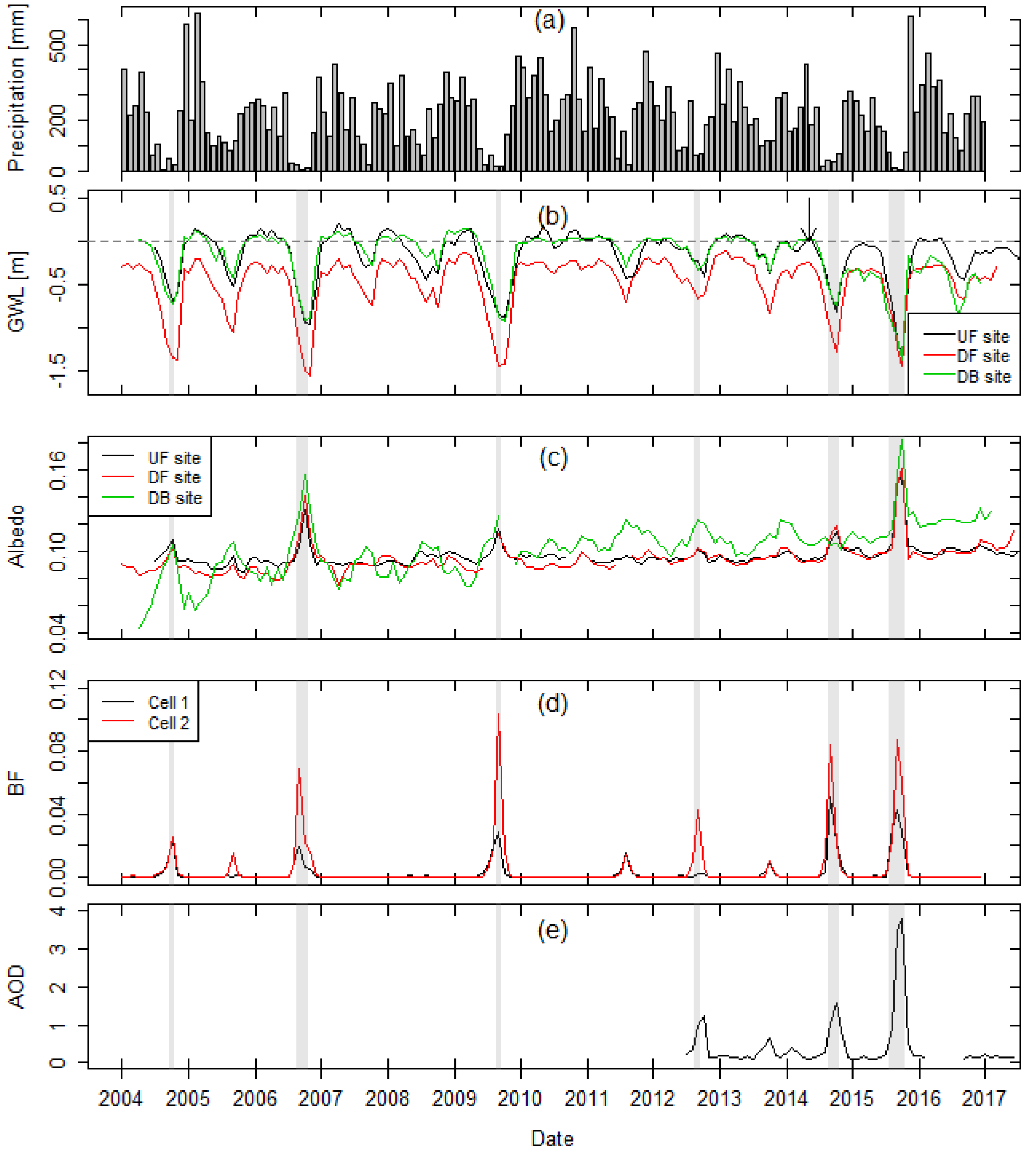
(a)
Precipitation [mm]
0
200
500
(b)
GWL [m]
0.5
-0.5
-1.5
UF site
DF site
DB site
(c)
Albedo
0.04
0.10
0.16
UF site
DF site
DB site
(d)
BF
0.00
0.04
0.08
0.12
Cell 1
Cell 2
(e)
AOD
0
1
2
3
4
2004
2005
2006
2007
2008
2009
2010
2011
2012
2013
2014
2015
2016
2017
Date

Figure 5

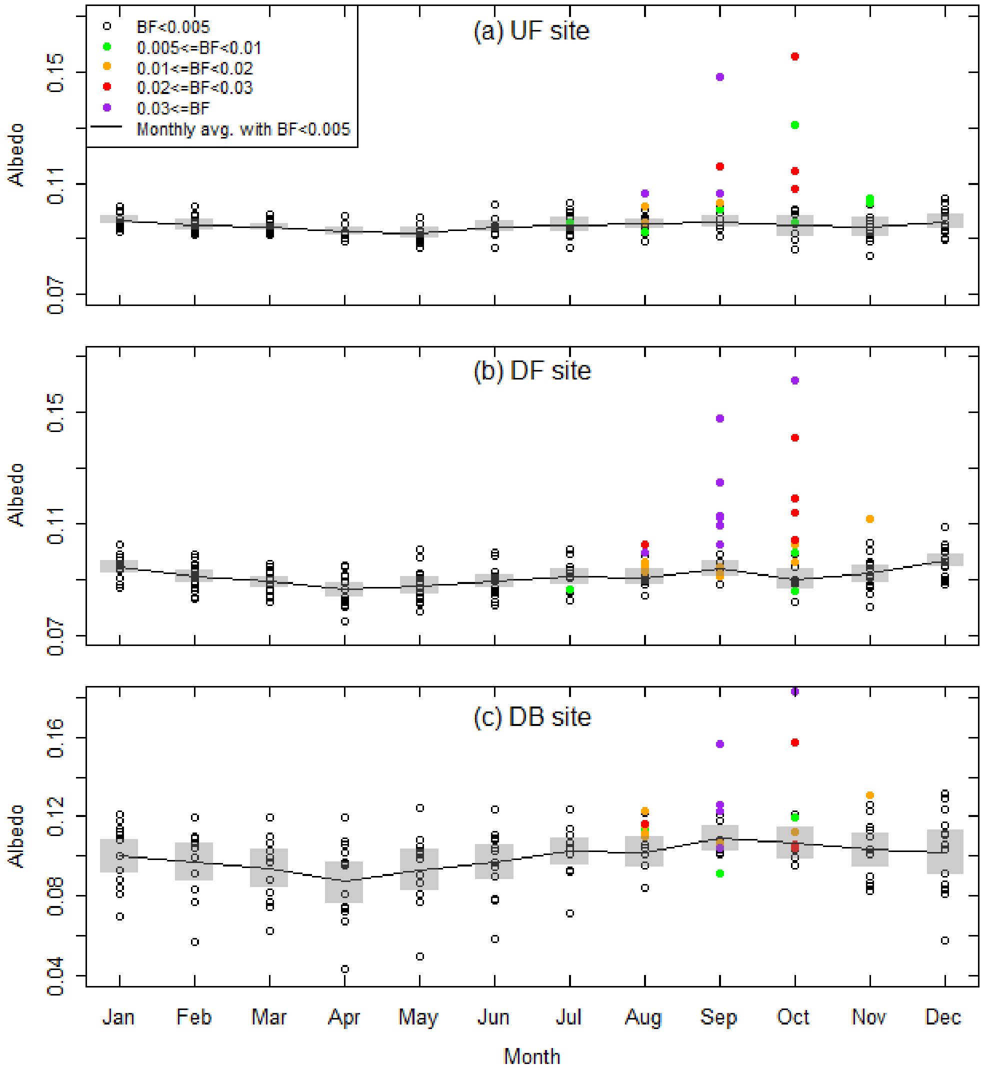
BF<0.005
0.005<=BF<0.01
0.01<=BF<0.02
0.02<=BF<0.03
0.03<=BF
Monthly avg. with BF<0.005
(a) UF site
(b) DF site
(c) DB site
Albedo
0.07
0.11
0.15
0.04
0.08
0.12
0.16
Jan
Feb
Mar
Apr
May
Jun
Jul
Aug
Sep
Oct
Nov
Dec
Month

Figure 6

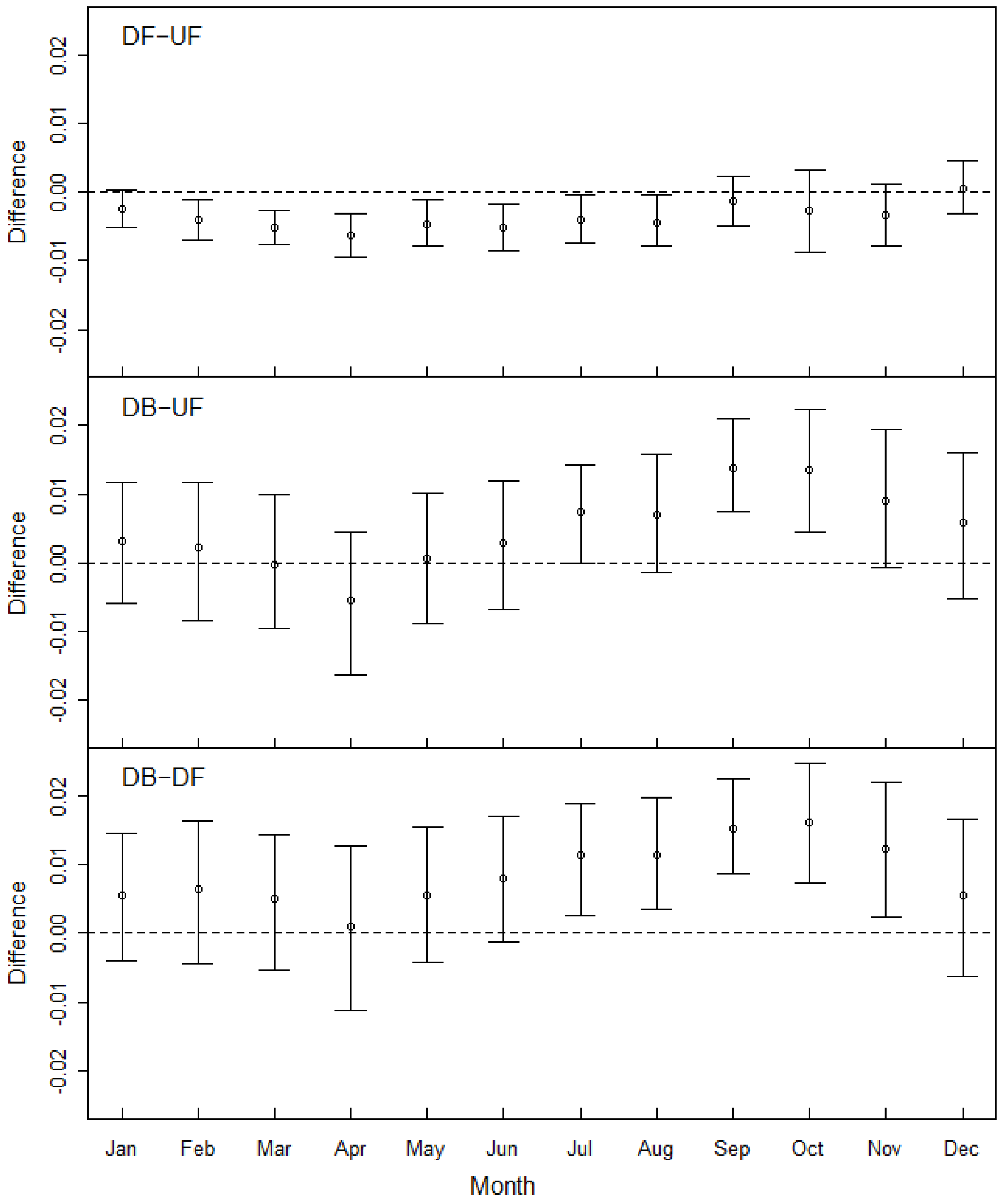
DF−UF
DB−UF
DB−DF
Difference
0.02
0.01
0.00
-0.01
-0.02
Jan
Feb
Mar
Apr
May
Jun
Jul
Aug
Sep
Oct
Nov
Dec
Month

Figure 7

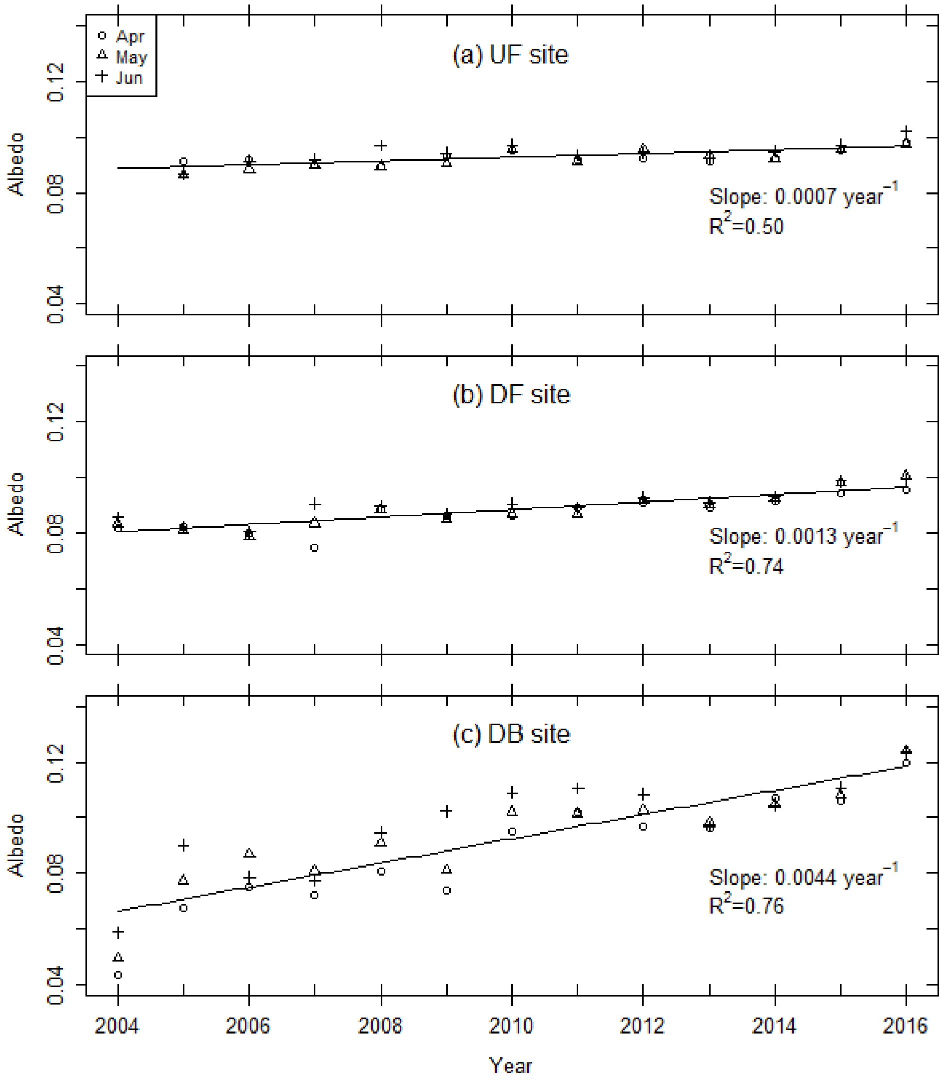

Apr
May
Jun
(a) UF site
Slope: 0.0007 $year^{-1}$
R^2=0.50
(b) DF site
Slope: 0.0013 $year^{-1}$
R^2=0.74
(c) DB site
Slope: 0.0044 $year^{-1}$
R^2=0.76
Albedo
0.04
0.08
0.12
2004
2006
2008
2010
2012
2014
2016
Year

722 Figure 8

723

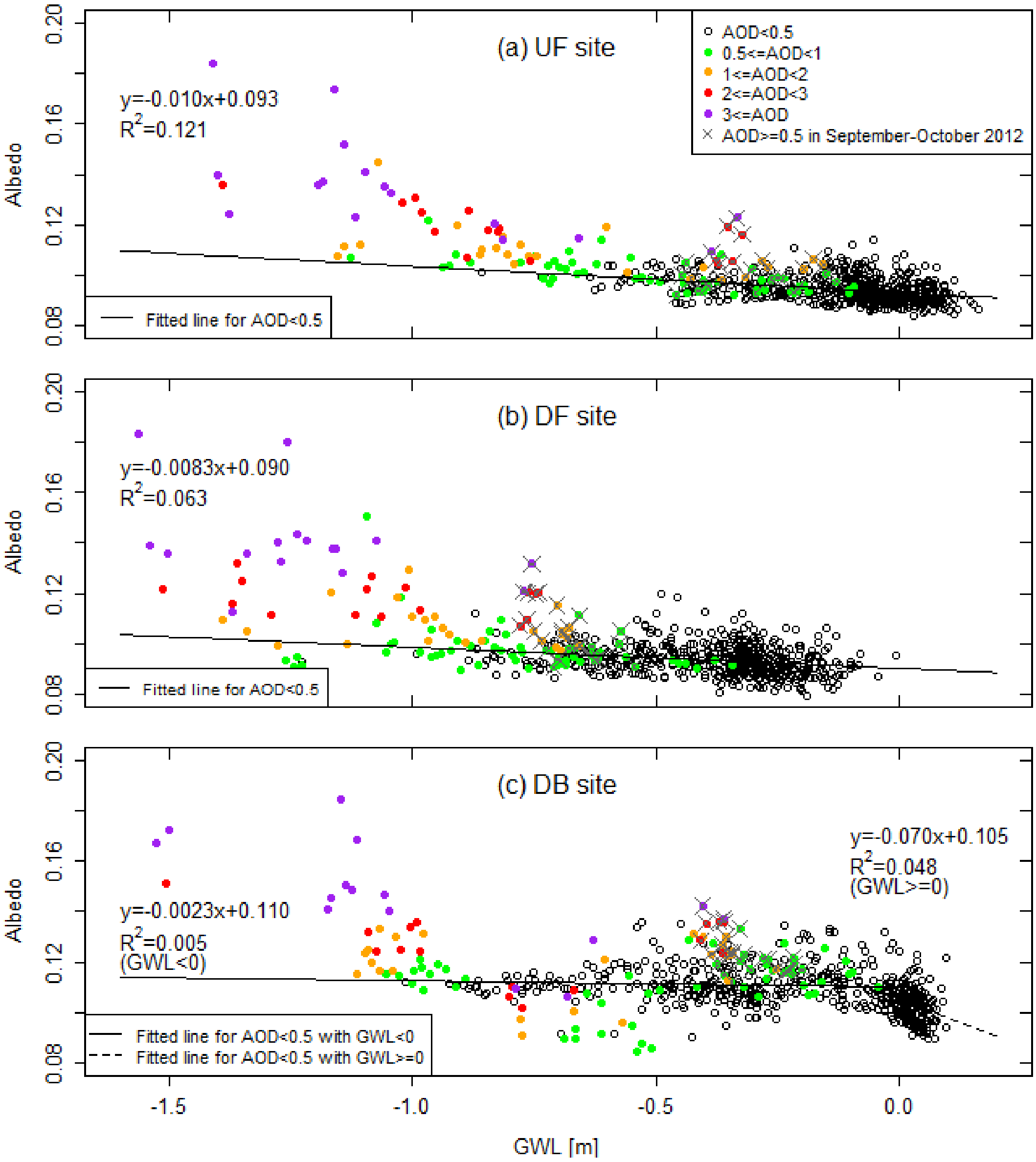

724

725

Figure 9

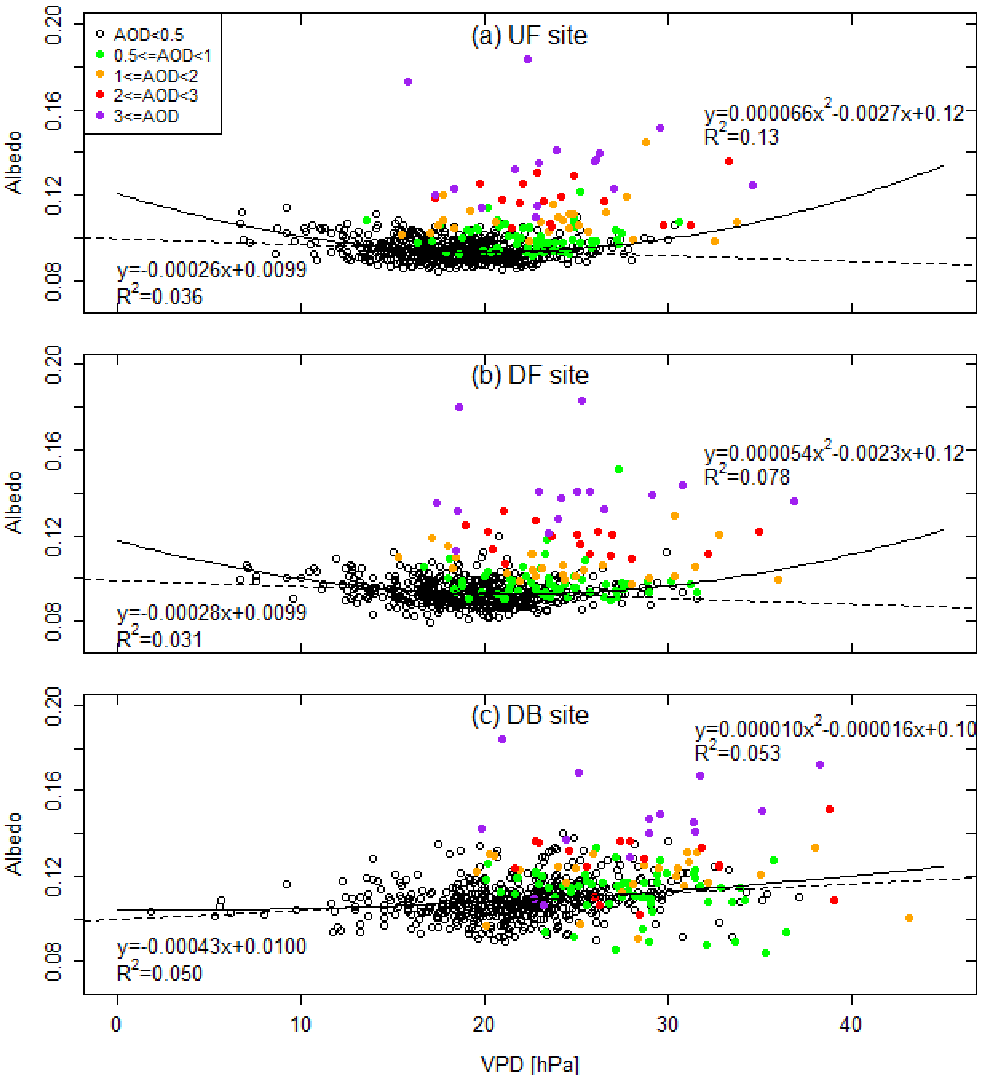
AOD<0.5
0.5<=AOD<1
1<=AOD<2
2<=AOD<3
3<=AOD
(a) UF site
y=0.000066x^2-0.0027x+0.12
R^2=0.13
y=-0.00026x+0.0099
R^2=0.036
(b) DF site
y=0.000054x^2-0.0023x+0.12
R^2=0.078
y=-0.00028x+0.0099
R^2=0.031
(c) DB site
y=0.000010x^2-0.000016x+0.10
R^2=0.053
y=-0.00043x+0.0100
R^2=0.050
Albedo
0.08
0.12
0.16
0.20
0
10
20
30
40
VPD [hPa]

Table 1

Site information

Site	UF	DF	DB
Geographical position	2.32ºS, 113.90ºE	2.35ºS, 114.04ºE	2.34ºS, 114.04ºE
Observation period	July 2004–June 2017	November 2001–June 2017	April 2004–February 2017
Canopy height (m)	23	26	0.2–1.8
Radiometer measurement height (m)	36.3	40.6	3.3 (Apr 2004–Mar2012) 6.8 (Mar 2012–Dec 2013) 13.6 (Dec 2013–Feb 2017)
Air temperature measurement height (m)	36.0	41.7	1.5

Table 2

Nomenclature

Notation	Unit	Definition
GWL	m	Groundwater level
S_u	W m^{-2}	Upward shortwave radiation
S_d	W m^{-2}	Downward shortwave radiation
BF		Burned fraction
VPD	hPa	Vapor pressure deficit
AOD		Aerosol optical depth
H_{obs}	m	Observation height
H_{cano}	m	Canopy height
β		Reflectance of the haze layer
γ		Absorbance of the haze layer
λ		Transmittance of the haze layer
α_{cano}		Albedo at the canopy
α_{obs}		Albedo at the observation height
x_L	m	Distance between observation height and canopy height
b_{ext}		Extinction coefficient
x_v	m	Visibility distance

Table 3

Comparison of albedo from forest and peatland sites.

Site type	Albedo	Reference
Tropical peatland	0.092–0.099	This study
Amazonia forest	0.114–0.115	Cescatti et al., 2012
Amazonia forest	0.12	Oliveira et al., 2019
Finnish peat bog	0.132	Gao et al., 2014
Open mesotrophic fen	0.137	Lohila et al., 2010
Open Finnish peatland	0.140	Kuusinen et al., 2013

Appendix

Monthly albedo (mean ± 1 standard deviation)

	UF	DF	DB
Jan	0.0968 ± 0.0030	0.0944 ± 0.0046	0.1000 ± 0.0166
Feb	0.0950 ± 0.0033	0.0909 ± 0.0049	0.0973 ± 0.0185
Mar	0.0942 ± 0.0025	0.0890 ± 0.0043	0.0940 ± 0.0174
Apr	0.0927 ± 0.0024	0.0863 ± 0.0057	0.0873 ± 0.0208
May	0.0922 ± 0.0034	0.0874 ± 0.0063	0.0929 ± 0.0185
Jun	0.0944 ± 0.0038	0.0892 ± 0.0055	0.0974 ± 0.0176
Jul	0.0951 ± 0.0044	0.0910 ± 0.0053	0.1028 ± 0.0127
Aug	0.0953 ± 0.0034	0.0906 ± 0.0043	0.1021 ± 0.0114
Sep	0.0961 ± 0.0032	0.0938 ± 0.0039	0.1090 ± 0.0086
Oct	0.0947 ± 0.0055	0.0901 ± 0.0053	0.1063 ± 0.0111
Nov	0.0944 ± 0.0060	0.0919 ± 0.0059	0.1032 ± 0.0154
Dec	0.0962 ± 0.0049	0.0967 ± 0.0056	0.1022 ± 0.0216